Article

Structural Mimicry of Two Cytochrome *b* Interhelical Loops Using Macrocycles Constrained by Oxazoles and Thiazoles

Yogendra Singh, Martin J. Stoermer, Andrew J. Lucke, Tom Guthrie, and David P. Fairlie

J. Am. Chem. Soc., **2005**, 127 (18), 6563-6572• DOI: 10.1021/ja0455300 • Publication Date (Web): 13 April 2005

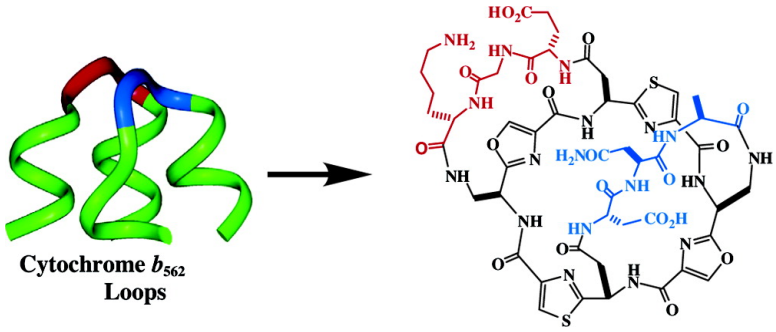

More About This Article

Additional resources and features associated with this article are available within the HTML version:

- Supporting Information
- Links to the 3 articles that cite this article, as of the time of this article download
- Access to high resolution figures
- Links to articles and content related to this article
- Copyright permission to reproduce figures and/or text from this article

View the Full Text HTML

J|A|C|S
ARTICLES
Published on Web 04/13/2005

Structural Mimicry of Two Cytochrome b_{562} Interhelical Loops Using Macrocycles Constrained by Oxazoles and Thiazoles

Yogendra Singh, Martin J. Stoermer, Andrew J. Lucke, Tom Guthrie, and David P. Fairlie*

Contribution from the Centre for Drug Design and Development, Institute for Molecular Bioscience, University of Queensland, Brisbane Qld 4072, Australia

Received July 26, 2004; E-mail: d.fairlie@imb.uq.edu.au

Abstract: A major chemical challenge is the structural mimicry of discontinuous protein surfaces brought into close proximity through polypeptide folding. We report the design, synthesis, and solution structure of a highly functionalized saddle-shaped macrocyclic scaffold, constrained by oxazoles and thiazoles, supporting two short peptide loops projecting orthogonally from the same face of the scaffold. This structural mimetic of two interhelical loops of cytochrome b_{562} illustrates a promising approach to structurally mimicking discontinuous loops of proteins.

Introduction

Current scientific, industrial, and medical uses of proteins and peptides are significantly limited by conformational flexibility, chemical and biological instability, low bioavailability, and high manufacturing costs.[1] Protein function is often mediated through small regions of folded polypeptide surfaces,[2] but short isolated peptides ($\leq$15 amino acids) corresponding to bioactive surfaces of proteins typically lack well-defined structure in water.[3] If such peptides could be restrained to shapes that structurally mimic protein surfaces, they could conceivably lead to cheaper, conformationally restrained, chemically stable, new nanomaterials with potential uses as supramolecular building blocks, artificial proteins, biological probes, drug leads, catalysts, and sensors. Toward this goal, small structural mimetics have been devised for peptide strands,[4] sheets,[4,5] helices,[6] turns,[7] and loops,[8] but there are very few examples of mimetics for discontinuous surfaces[9] of proteins, such as multiple loops (Figure 1)[10] formed by residues well separated in sequence but brought close together in three-dimensional space by polypeptide folding. To test a promising approach to multi-loop mimicry, we chose to structurally mimic two interhelical tripeptide loops of the well-studied[11] cytochrome b_{562} (Figure 1), its loops being fairly rigidly positioned at the ends of the helices and well defined in the crystal structure.[12]

(1) (a) Milner-White, E. J. *Trends Pharmacol. Sci.* **1989**, *10*, 70−74. (b) West, M. L.; Fairlie, D. P. *Trends Pharmacol. Sci.* **1995**, *16*, 67−75. (c) Lee, H. J. *Arch. Pharm. Res.* **2002**, *25*, 572−584. (d) Witt, K. A.; Gillespie, T. J.; Huber, J. D.; Egleton, R. D.; Davis, T. P. *Peptides* **2001**, *22*, 2329−2343. (e) Topp, E. M. *Med. Chem. Res.* **1997**, *7*, 493−508. (f) Chan, O. H.; Stewart, B. H. *Drug Discovery Today* **1996**, *11*, 461−473.

(2) (a) Giannis, A. *Angew. Chem., Int. Ed. Engl.* **1993**, *32*, 1244−1267. (b) Gante, J. *Angew. Chem., Int. Ed. Engl.* **1994**, *33*, 1699−1720. (c) Schneider, J. P.; Kelly, J. W. *Chem. Rev.* **1995**, *95*, 2169−2187. (d) Fairlie, D. P., West, M. L.; Wong, A. K. *Curr. Med. Chem.* **1998**, *5*, 29−62.

(3) (a) Zimm, B.; Bragg, J. *J. Chem. Phys.* **1959**, *31*, 526−535. (b) Scholtz, J. M.; Baldwin, R. L. *Annu. Rev. Biophys. Biomol. Struct.* **1992**, *21*, 95−118. (c) Dyson, H. J.; Wright, P. E. *Ann. Rev. Biophys. Biophys. Chem.* **1991**, *20*, 519−538.

(4) (a) Glenn, M. P.; Fairlie, D. P. *Mini-Rev. Med. Chem.* **2002**, *2*, 433−445. (b) Loughlin, W. A.; Tyndall, J. D. A.; Glenn, M. P.; Fairlie, D. P. *Chem. Rev.* **2004**, *104*, 6085−6117.

(5) Sheets: (a) Nowick, J. S. *Acc. Chem. Res.* **1999**, *32*, 287−296. (b) Moriuchi, T.; Hirao, T. *Chem. Soc. Rev.* **2004**, *33*, 294−301.

(6) Helices: (a) Andrews, M. J. I.; Tabor, A. B. *Tetrahedron* **1999**, *55*, 11711−11743. (b) Taylor, J. W. *Biopolymers* **2002**, *66*, 49−75. (c) Kelso, M. J.; Hoang, H.; Appleton, T. G.; Fairlie, D. P. *J. Am. Chem. Soc.* **2000**, *122*, 10488−10489. (d) Kelso, M. J.; Hoang, H. N.; Oliver, W. N.; Sokolenko, N.; March, D. R.; Appleton, T. G.; Fairlie, D. P. *Angew. Chem, Int. Ed.* **2003**, *42*, 421−424. (e) Kelso, M. J.; Beyer, R. L.; Hoang, H. N.; Lakdawala, A. S.; Snyder, J. P.; Oliver, W. P.; Robertson, T. A.; Appleton, T. G.; Fairlie, D. P. *J. Am. Chem. Soc.* **2004**, *126*, 4828−4842. (f) Shepherd, N. E.; Abbenante, G.; Fairlie, D. P. *Angew. Chem., Int. Ed.* **2004**, *43*, 2687−2690. (g) Fasan, R.; Dias, R. L. A.; Moehle, K.; Zerbe, O.; Vrijbloed, J. W.; Obrecht, D.; Robinson, J. A. *Angew. Chem., Int. Ed.* **2004**, *43*, 2109−2112. (h) Shepherd, N. E.; Hoang, H. N.; Abbenante, G.; Fairlie, D. P. *J. Am. Chem. Soc.* **2005**, *127*, 2974−2983.

(7) Turns: (a) Hruby, V. J.; al-Obeidi, F.; Kazmierski, W. *Biochem. J.* **1990**, *268*, 249−262. (b) Toniolo, C. *Int. J. Pept. Protein Res.* **1990**, *35*, 287−300. (c) Hruby, V. J.; Sharma, S. D. *Curr. Opin. Biotechnol.* **1991**, *2*, 599−605. (d) Holzemann, G. *Kontakte (Darmstadt)* **1991**, 3−12 and 55. (e) Giannis, A. *Angew. Chem., Int. Ed. Engl.* **1993**, *32*, 1244−1267. (f) Fairlie, D. P., Abbenante, G.; March, D. R. *Curr. Med. Chem.* **1995**, *2*, 654−686. (g) Jones, R. M.; Boatman, P. D.; Semple, G.; Shin, Y. J.; Tamura, S. Y. *Curr. Opin. Pharmacol.* **2003**, *3*, 530−543. (h) Kee, S.; Jois, S. D. S. *Curr. Pharm. Des.* **2003**, *9*, 1209−1224.

(8) Loops: (a) Bisang, C.; Weber, C.; Robinson, J. A. *Helv. Chim. Acta* **1996**, *79*, 1825−1841. (b) Pfeifer, M. E.; Robinson, J. A. *Chem. Commun.* **1998**, 1977−1978. (c) Bisang, C.; Jiang, L.; Freund, E.; Emery, F.; Bauch, C.; Matile, H.; Pluschke, G.; Robinson, J. A. *J. Am. Chem. Soc.* **1998**, *120*, 7439−7449. (d) Favre, M.; Moehle, K.; Jiang, L.; Pfeiffer, B.; Robinson, J. A. *J. Am. Chem. Soc.* **1999**, *121*, 2679−2685. (e) Wittelsberger, A.; Keller, M.; Scarpellino, L.; Patiny, L.; Acha-Orbea, H.; Mutter, M *Angew. Chem., Int. Ed.* **2000**, *39*, 1111−1115. (f) Peri, F.; Grell, D.; Dumy, P.; Yokokawa, Y.; Welzenbach, K.; Weitz-Schmidt, G.; Mutter, M. *J. Pept. Sci.* **1999**, *5*, 313−322. (g) Mathieu, M.; Lehmann, C.; Razaname, A.; Tuchscherer, G. *Lett. Pept. Sci.* **1997**, *4*, 95−100.

(9) Discontinuous surfaces: (a) Mutter, M.; Vuillemeumier, S. *Angew. Chem., Int. Ed. Engl.* **1989**, *28*, 535−676. (b) Hauert, J.; Fernandez-Carneado, J.; Michielin, O.; Mathieu, S.; Grell, D.; Schapira, M.; Spertini, O.; Mutter, M.; Tuchscherer, G.; Kovacsovics, T. *ChemBioChem* **2004**, *5*, 856−864.

(10) Multiloops: (a) Mutter, M.; Dumy, P.; Garrouste, P.; Lehmann, C.; Mathieu, M.; Peggion, C.; Peluso, S.; Razaname, A.; Tuchscherer, G. *Angew. Chem., Int. Ed. Engl.* **1996**, *35*, 1482−1485. (b) Hamuro, Y.; Calama, M. C.; Park, H. S.; Hamilton, A. D. *Angew. Chem., Int. Ed. Engl.* **1997**, *36*, 2680−2683. (c) Peluso, S.; Dumy, P.; Eggleston, Im.; Garrouste, P.; Mutter, M. *Tetrahedron* **1997**, *53*, 7231−7236. (d) Peluso, S.; Dumy, P.; Nkubana, C.; Yokokawa, Y.; Mutter, M. *J. Org. Chem.* **1999**, *64*, 7114−7120. (e) Reineke, U.; Schneider-Mergener, J. *Angew. Chem., Int. Ed.* **1998**, *37*, 769−771.

(11) Jones, D. D.; Barker, P. D. *ChemBioChem* **2004**, *5*, 964−971.

(12) Hamada, K.; Bethge, P. H.; Mathews, F. S. *J. Mol. Biol.* **199**5, *247*, 947−962.

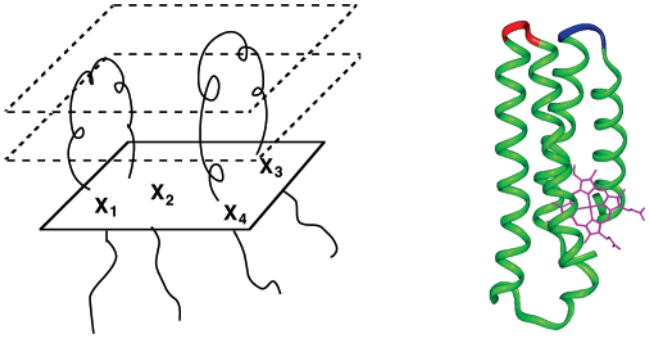

Figure 1. Discontinuous loop surfaces of proteins. (left) Theoretical scaffold planes that intersect with protein loops define dimensions of both peptide loops and putative scaffold onto which they will be grafted, providing scaffold coordinates (X_{1-4}) for attachment of loops; (right) crystal structure[12] of cytochrome b_{562} (pdb: 256b) showing helices (green), heme (purple), and the specific interhelix tripeptide loop sequences (red and blue) to be mimicked.

The first objective was to develop a scaffold, highly functionalized at appropriate positions (e.g., X_1, X_2, X_3, X_4 in Figure 1) to support peptide sequences corresponding to two tripeptide loops of cytochrome b_{562}. The scaffold needed to have the capacity to direct the attached loops orthogonally from the same face of the scaffold into adjacent three-dimensional space, and to be able to hold the loops in reasonable proximity to one another. Inspired by Nature's use of heterocyclic five-membered ring constraints such as oxazole/oxazoline/thiazole/thiazoline/thiazolidine (e.g.,**1**−**3**, X = O, S) to regulate peptide shapes in fungi, bacteria, marine organisms, and plants,[13] we have been exploring structural effects of such constraints in cyclic peptides.[14−18] We[14−17] and others[19] have synthesized a number of such constrained macrocycles, those containing oxazole/thiazole dipeptide surrogates (e.g., **4**, **5**) tending to be rigid and psuedo-planar, the amino acid side-chains projecting from either face depending on the R- or S-configuration at the α-carbon. Molecular modeling studies[17,18] suggested that such cyclic peptides, with predetermined tethering points, might be ideal scaffolds on which to mount peptide helices or loops to structurally mimic discontinuous protein surfaces.

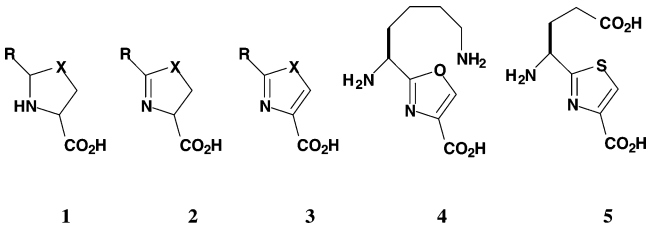

1 **2** **3** **4** **5**

We recently reported the use of **4** and **5** to synthesize the highly functionalized scaffold **6**.[17] Controlled condensation of lysine with glutamate side chains in **6** enabled stereoselective ring closure to form the novel tris-macrocyclic molecule **7**,[17] a prototype for two-loop protein surface mimetics. We now demonstrate that macrocycle **6** has the appropriate dimensions and side-chain directionality to be a suitable scaffold for building larger and more complex tris-macrocyclic compounds as prospective protein loop mimetics. However, condensation of the unequal length side chains of the Lys and Glu residues in **6** had the effect in **7** of staggering the loops with respect to one another.[17] We therefore decided to modify **6**, replacing Lys with Dap (2,3-diaminopropanoic acid) and Glu with Asp, to create side chains of uniform and reduced length. Herein, we specifically describe the design, synthesis, and three-dimensional solution structure, determined in water by 2D ^{1}H NMR spectroscopy, of the densely functionalized tris-macrocycle **8**. We also compare this structure with the corresponding interhelical loops in the crystal structure of cytochrome b_{562}. We show that compound **8** projects two tripeptide loops perpendicularly from the same face of the constrained macrocyclic analogue of scaffold **6**, due to like chirality of all four amino acids inserted between oxazoles/thiazoles, and we reveal that **8** is a successfully designed structural mimetic for the two interhelical loops of cytochrome b_{562}.

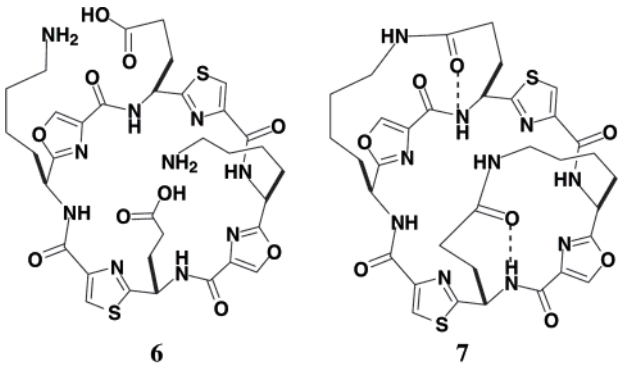

6 **7**

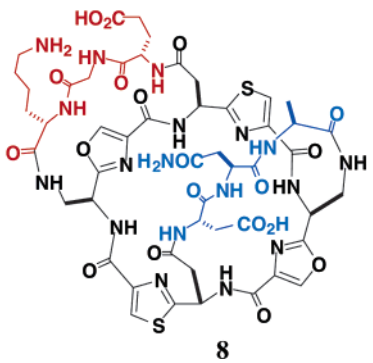

8

(13) (a) Wipf, P. *Chem. Rev.* **1995**, *95*, 2115−2134. (b) Ishida, T.; Inoue, M.; Hamada, Y.; Kato, S.; Shiori, T. *J. Chem. Soc., Chem. Commun.* **1987**, 370−371. (c) Todorova, A. K.; Juttner, F.; Linden, A.; Pluss, T.; von Philipsborn, W. *J. Org. Chem.* **1995**, *60*, 7891−7895. (d) Toske, S. G.; Fenical, W. *Tetrahedron Lett.* **1995**, *36*, 8355−8. (e) Ireland, C. M.; Scheuer, P. J. *J. Am. Chem. Soc.* **1980**, *102*, 5688−5691. (f) Sowinski, J.; Toogood, P. L. *Tetrahedron Lett.* **1995**, *36*, 67−70. (g) Fate, G. D.; Benner, C. P.; Grode, S. H.; Gilbertson, T. J. *J. Am. Chem. Soc.* **1996**, *118*, 11363−11368. (h) McGeary, R. P.; Fairlie, D. P. *Curr. Opin. Drug Discuss. Dev.* **1998**, *1*, 208−217. (i) Lewis, J. R. *Nat. Prod. Rep.* **2002**, *19*, 223−258.
(14) Abbenante, G.; Fairlie, D. P.; Gahan, L. R.; Hanson, G. R.; Pierens, G.; van den Brenk, A. L. *J. Am. Chem. Soc.* **1996**, *118*, 10384−10388.
(15) Sokolenko, N.; Abbenante, G.; Scanlon, M. J.; Jones, A.; Gahan, L. R.; Hanson, G. R.; Fairlie, D. P. *J. Am. Chem. Soc.* **1999**, *121*, 2603−2604.
(16) Singh, Y.; Sokolenko, N.; Kelso, M. J.; Gahan, L. R.; Abbenante, G.; Fairlie, D. P. *J. Am. Chem. Soc.* **2001**, *123*, 333−334.
(17) Singh, Y.; Stoermer, M. J.; Lucke, A. J.; Glenn, M. P.; Fairlie, D. P. *Org. Lett.* **2002**, *4*, 3367−3370.
(18) Lucke, A. J.; Tyndall, J. D. A.; Singh, Y.; Fairlie, D. P. *J. Mol. Graphics Modell.* **2003**, *21*, 341−355.
(19) (a) Wipf, P.; Venkatraman, S. *J. Org. Chem.* **1995**, *60*, 7224−7229. (b) Wipf, P.; Fritch, P. C.; Geib, S. J.; Sefler, A. M. *J. Am. Chem. Soc.* **1998**, *120*, 4105−4112. (c) Mink, D.; Mecozzi, S.; Rebek, J., Jr. *Tetrahedron Lett.* **1998**, *39*, 5709−5712. (d) Haberhauer, G.; Somogyi, L.; Rebek, J., Jr. *Tetrahedron Lett.* **2000**, *41*, 5013−5016. (e) Somogyi, L.; Haberhauer, G.; Rebek, J., Jr. *Tetrahedron Lett.* **2001**, *57*, 1699−1708. (f) Boss, C.; Rasmussen, P. H.; Wartini, A. R.; Waldvogel, S. R. *Tetrahedron Lett.* **2000**, *41*, 6327−6331. (g) Wipf, P.; Miller, C. P.; Grant, C. M. *Tetrahedron* **2000**, *56*, 9143−9150. (h) Bertram, A.; Blake, A. J.; de Turiso, F. G. L.; Hannam, J. S.; Jolliffe, K. A.; Pattenden, G.; Skae, M. *Tetrahedron* **2003**, *59*, 6979−6990.

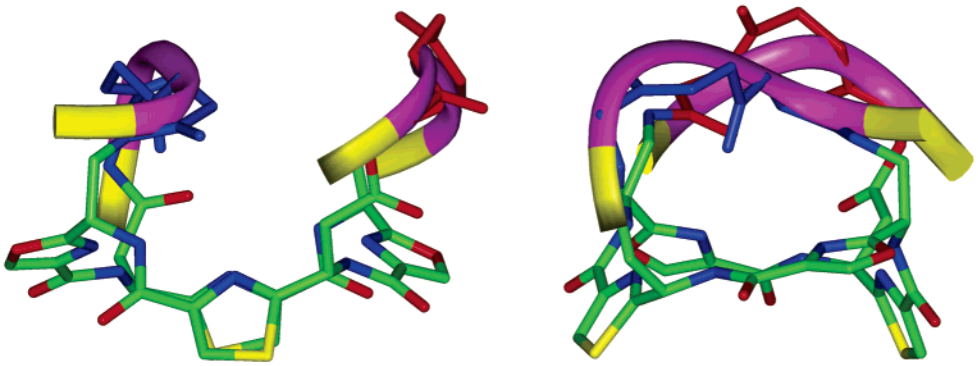

Figure 2. Design of a protein surface mimetic. End (left) and side (right) views of superimposition of modeled 2-loop mimetic **8**, featuring a side-chain modified scaffold **6** (green) condensed with tripeptides Asp−Asn−Ala (blue) and Glu−Gly−Lys (red) to form loops, and the corresponding interhelix loop sequences Asp21−Asn22−Ala23 and Glu81−Gly82−Lys83 (purple ribbons) from the crystal structure of cytochrome b_{562}.

Results

Design of Mimetic for Cytochrome b_{562} Loops. Computer modeling was first used to predict whether scaffold **6** might be of approximate size and shape to support peptides that could structurally mimic loop regions of a protein. The oxidized form of cytochrome b_{562}, a monomeric heme-binding four α-helix bundle protein from the periplasm of *Escherichia coli*, was chosen for mimicry on the basis that it represents a typical 4-helix bundle that fairly rigidly defines the locations of its interhelical loops.[12] Specifically its two interhelical loops Asp21−Asn22−Ala23 (blue) and Glu81−Gly82−Lys83 (red) (Figure 1b) that connect α-helices α1-α2 and α3-α4, respectively, were grafted in silico from its reported high-resolution crystal structure (b256)[12] onto the energy minimized, and side-chain modified, scaffold **6** using InsightII. We were particularly conscious of the fact that the tripeptide loops in cytochrome b_{562} were directly tethered to the ends of the four helices, and so we wished to use as short a linker as possible between the loops and the scaffold in our target molecule.

Tricyclic construct **8** was energy minimized before superimposition with template forcing of all 24 tripeptide backbone heavy atoms (N, Cα, C, O) onto the corresponding tripeptide atoms of cytochrome b_{562}. Template forcing (minimization with pairwise atom force restraints) was used because it can be useful for identifying conformations that are of biological relevance. Figure 2 shows the resulting conformation of **8** after template forcing using default parameters, the scaffold (green) being of approximately the correct size and geometry to project the loops orthogonally from the pseudo-planar scaffold, demonstrated by the good match (RMSD 1.21 Å) between the atoms of the tripeptide components of the tris-macrocyclic construct (green) and the cytochrome (purple ribbons).

Synthesis of Tris-macrocycle 8. The synthesis of **8** involved first creating a scaffold **13** (a side-chain modified analogue of **6**) with four differentially protected Asp/Dap side chains (Scheme 1), followed by grafting the tripeptide chains onto the scaffolds and cyclizing them. This approach involved sequentially forming the two loops, coupling one tripeptide to the scaffold and cyclizing it, and then coupling the scaffold−loop conjugate to the second tripeptide which was subsequently cyclized to produce **8** (Scheme 2).

Synthesis of Macrocyclic Scaffold 13. Scaffold **13**, with side-chain functional groups differentially protected, was synthesized using the dipeptide surrogates Boc-L-Dap(Fmoc)(Ox)-OH (**9a**) (Boc is *tert*-butoxycarbonyl, Ox is oxazole), Boc-L-Dap(Alloc)(Ox)-OH (**9b**) (Alloc is allyloxycarbonyl), H-L-Asp(O*t*Bu)(Thz)-OH (**10a**) (Thz is thiazole), and H-L-Asp(OAllyl)(Thz)-OtBu (**10b**), in turn respectively prepared from oxazole **9c** and thiazoles **10c** and **10d**.

Oxazole **9c** was conveniently synthesized from the dipeptide Boc-L-Dap(Z)Ser-OMe (Z is benzyloxycarbonyl) by cyclodehydration using diethylaminosulfur trifluoride (DAST)[20] followed by oxidation with a mixture of bromotrichloromethane and a strong base 1,8-diazabicyclo[5.4.0]undec-7-ene (DBU).[17] It was necessary to replace the Z protecting group of **9c** with Alloc and Fmoc groups, respectively, for compatibility with subsequent steps. This was accomplished using a deprotection and reprotection strategy. Catalytic hydrogenolysis of the side chain Z protecting group followed by reaction of the free amino group with allyl chloroformate in the presence of DIPEA (diisopropylethylamine) as base, and hydrolysis of the methyl ester with LiOH gave Boc-L-Dap(Alloc)(Ox)-OH (**9b**). Boc-L-Dap(Fmoc)(Ox)-OH (**9a**) was easily obtained from **9c** after sequential hydrolysis of the methyl ester, removal of the Z protecting group by catalytic hydrogenolysis, and subsequent treatment of the free amino acid (**9d**) with Fmoc-OSu.

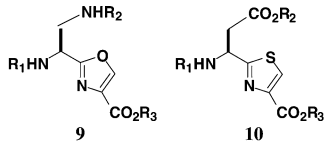

9 **10**

9a R_1 = Boc, R_2 = Fmoc, R_3 = H
9b R_1 = Boc, R_2 = Alloc, R_3 = H
9c R_1 = Boc, R_2 = Z, R_3 = Me
9d R_1 = Boc, R_2 = H, R_3 = H

10a R_1 = H, R = *t*Bu, R_3 = H
10b R_1 = H, R = Allyl, R_3 = *t*Bu
10c R_1 = Fmoc, R = *t*Bu, R_3 = Et
10d R_1 = Fmoc, R =Allyl, R_3 =*t*Bu

Thiazoles **10c** and **10d** were synthesized from commercially available amino acids Fmoc-L-Asp(OtBu)-OH and Fmoc-L-Asp-(OAllyl)-OH, following conversion to the corresponding thioamides using Lawesson's reagent and a modified Hantzch synthesis[16] using ethyl bromopyruvate and *tert*-butyl bromopyruvate, respectively (Supporting Information). Selective removal of the Fmoc protecting group of **10d** with piperidine in dichloromethane furnished thiazole **10b** [H-Glu(OAllyl)(Thz)-OtBu]. Simultaneous removal of Fmoc and ethyl ester groups from thiazole **10c** using LiOH gave **10a** [H-Asp(O*t*Bu)(Thz)-OH] in 96% yield.

(20) Phillips, A. J.; Uto, Y.; Wipf, P.; Reno, M. J.; Williams, D. R. *Org. Lett.* **2000**, *2*, 1165−1168.

Scheme 1. Synthesis of Differentially Protected Scaffold **13**[a]

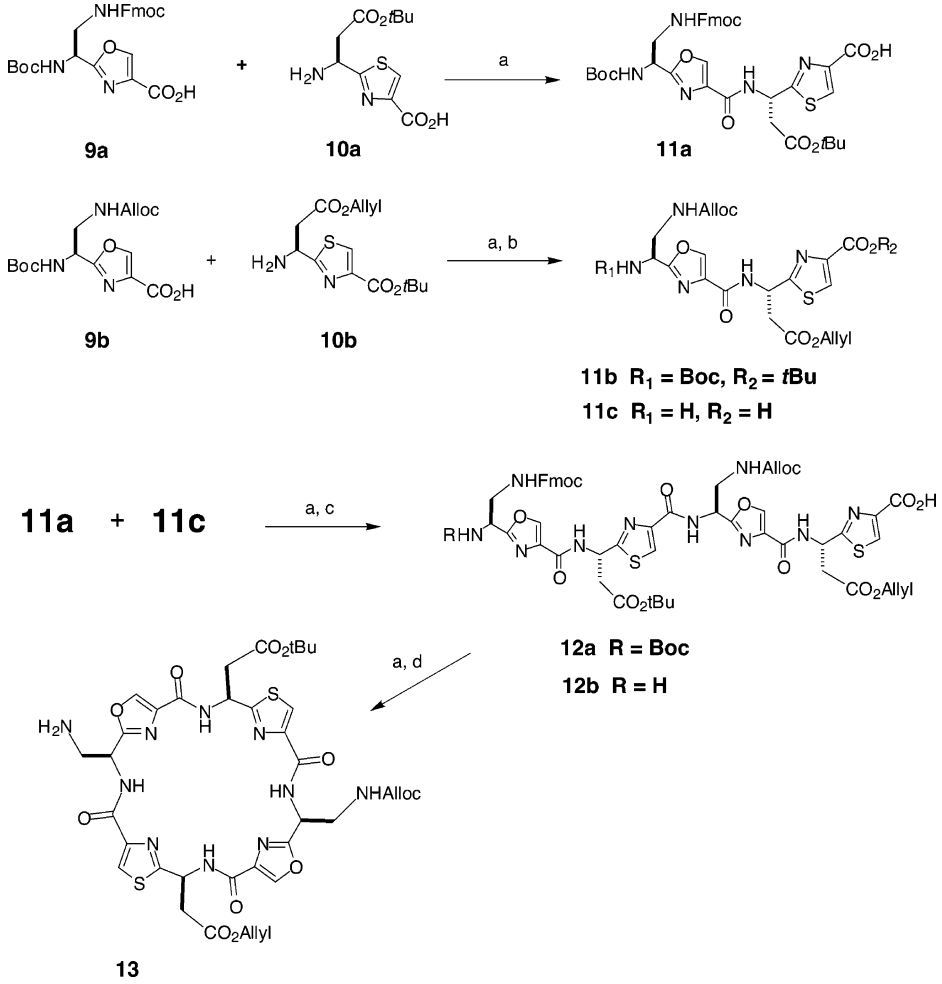

[a] Reagents: (a) BOP, DIPEA, DMF, room temperature; (b) TFA/DCM, room temperature; (c) formic acid, room temperature; (d) 30% piperidine/DCM, room temperature.

Pairs of dipeptide surrogates **9a** and **10a**, and **9b** and **10b**, were elaborated to tetrapeptide analogues **11a** [Boc-Dap(Fmoc)-(Ox)Asp(OtBu)(Thz)-OH] and **11b** [Boc-Dap(Alloc)(Ox)Asp-(OAllyl)(Thz)-OtBu], respectively (Scheme 1). Tetrapeptide analogue **11b** was then treated with TFA (trifluoroacetic acid) and coupled to **11a** using BOP ([benzotriazol-1-yl-oxytris-(dimethylamino) phosphonium] hexafluorophosphate) reagent in the presence of DIPEA to give linear octapeptide analogue **12a** in high yield (91%). Selective removal of the Boc protecting group of **12a** using neat formic acid gave **12b** with free N- and C-terminal functional groups required for final cyclization. Macrolactamization of **12b** under high dilution (1×10^{-3} M) with BOP using DIPEA and DMF (*N*,*N*-dimethylformamide) resulted in a high isolated yield of cyclic octapeptide **13** (81%), after removal of the Dap side-chain Fmoc protecting group (Scheme 1). Cyclization of **12b** is favored over cyclooligomerization by the presence of four turn-inducing heterocyclic oxazole/thiazole constraints, which preorganize it for cyclization.[16]

Elaboration of 13 to 8. The next step in the synthesis of tris-macrocycle **8** involved the grafting of the two tripeptide loops onto scaffold **13**. We developed a strategy where the C-terminus of the tripeptides was coupled to the scaffold Dap side chains, prior to intramolecular loop formation by condensation of the N-terminus of the tripeptides with the carboxylic acid side chains of the scaffold. Tripeptides Boc-Glu(OcHx)-GlyLys(Z)-OH and Boc-Asp(OcHx)Asn(NHTrt)-Ala-OH were obtained by synthesis on TCP resin using Fmoc protocols and subsequent cleavage with 1% TFA in dichloromethane as solvent. The coupling of the tripeptide Boc-Glu(OcHx)GlyLys-(Z)-OH to the scaffold **13** was best achieved by using DPPA (diphenylphosphoryl azide)/DIPEA at low temperature (~5 °C), with no epimerization detected at the lysine α-carbon atom of the tripeptide.

Simultaneous removal of Boc and *tert*-butyl groups with TFA in the presence of scavengers (water and triisopropylsilane) led to isolation of compound **14** in 88% yield. Intramolecular loop formation under dilute conditions (9×10^{-4} M) and at low temperature (~5 °C) in DMF using DPPA gave compound **15** in 86% yield, after simultaneous cleavage of Alloc and allyl ester groups with $Pd(PPh_3)_4$ in the presence of 1,3-dimethyl-barbituric acid and acetic acid in dichloromethane as solvent. The use of DPPA instead of DOP avoids formation of hydroxybenzotriazole which tends to be trapped in the cycle.[15]

Coupling of the second tripeptide Boc-Asp(OcHx)Asn-(NHTrt)Ala-OH to **15** was challenging as it required activation of a peptidyl alanine residue which, unlike N-terminus protected amino acid, is prone to epimerization at the α-carbon atom. In addition, both the amine and the carboxylic acid functionalities in **15** are not protected. The coupling was achieved with minimal

Scheme 2. Synthesis of Tris-macrocyclic Protein Mimetic **8**[a]

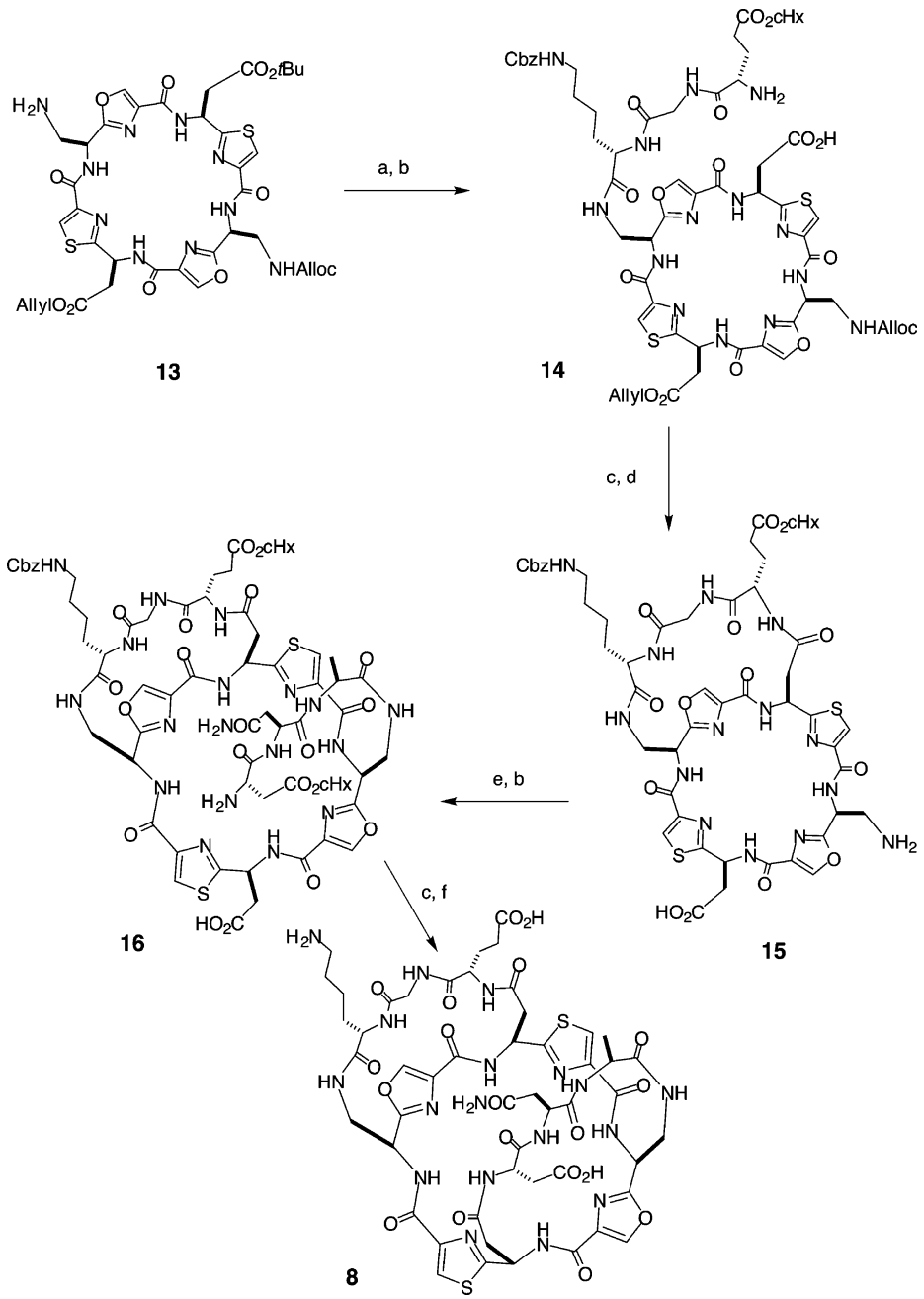

[a] Reagents: (a) Boc-Glu(OcHx)GlyLys(Z)-OH, DPPA, DIPEA, DMF, ~5 °C; (b) TFA, TIPS, H_2O; (c) DPPA, DIPEA, DMF (1×10^{-3} M), ~5 °C; (d) $Pd(PPh_3)_4$, 1,3-dimethylbarbituric acid, AcOH, DCM, N_2, dark, room temperature; (e) Boc-Asp(OcHx)Asn(NHTrt)Ala-OH, DPPA, DIPEA, DMF, ~5 °C; (f) HF, *p*-cresol.

racemization (~5%) when the tripeptide was activated with DPPA[21] in the presence of just the required amount of DIPEA as base for about 15 min at ~5 °C prior to addition of **15**; however, the reaction was very slow. This is not surprising in view of the fact that the reactive functional groups on the Dap-(Ox) and Asp(Thz) side chains are only 2 bond lengths from the scaffold, sterically interfering with the intermolecular reaction. Compound **16** was isolated in 65% yield after stirring the mixture of **15**, Boc-Asp(OcHx)Asn(NHTrt)Ala-OH, and DPPA in the presence of DIPEA as base and DMF as solvent for 4 days followed by treatment with TFA. Conversion to **8** involved stirring **16** with DPPA and DIPEA in DMF for 8 days to produce the fully protected tris-macrocycle, before removing the cyclohexyl and Z protecting groups with HF in the presence of *p*-cresol as scavenger and purification to **8** by rp-HPLC (35% isolated yield).

Solution Structure of Scaffold 6. The macrocycle in scaffold **6** possessed a small measure of structure in water. The diagnostic large $^3J_{\alpha H-NH}$ coupling constants for the Glu(Thz) (8.9 Hz) and Lys(Ox) (9.1 Hz), when used as dihedral restraints in an XPLOR-based NMR solution structure determination, resulted in a moderately defined square macrocycle (RMSD 0.8 Å) with randomly distributed side chains. The 20 lowest energy structures (Figure 3) contained no NOE distance (>0.1 Å) or dihedral

(21) Eichler, J.; Lucka, A. W.; Pinilla, C.; Houghten, R. A. *Mol. Diversity* **1996**, *1*, 233−240.

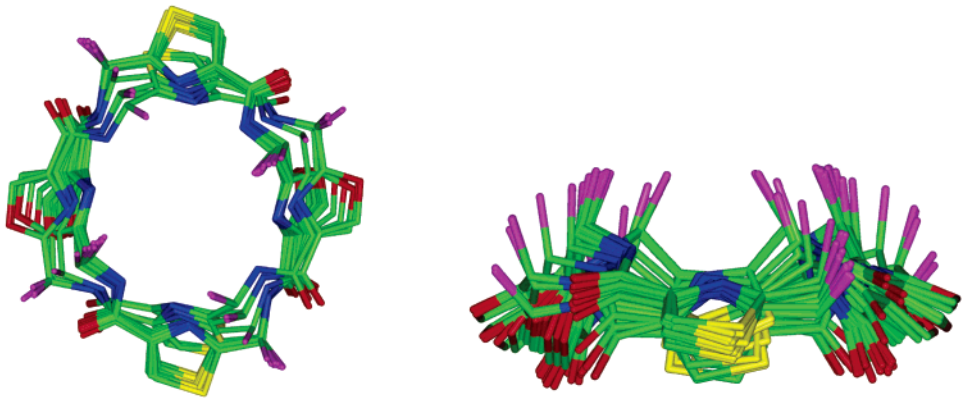

Figure 3. Top and side views of the 20 lowest energy, NMR-derived, solution structures of scaffold **6** (β carbons colored purple, remaining side-chain atoms not displayed for clarity).

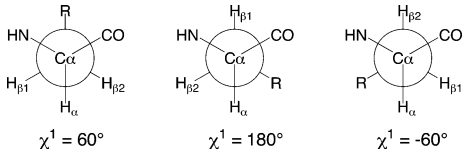

Figure 4. Newman projections of Cα−Cβ bonds showing the three possible χ^1 rotamers. χ^1 was assigned −60° for Asp(Thz) and +60° for Dap(Ox).

angle (>3°) violations. There were a number of weak NOEs, notably between scaffold components Lys(Ox) Hβs and Glu(Thz) NH, and between Glu(Thz) Hβs and Lys(Ox) NH, that could not be unambiguously assigned due to the symmetrical nature of the molecule. These were omitted from the structure calculation, so as not to bias the macrocycle fold. Variable-temperature NMR experiments (Supporting Information, Figure S1) indicated that the four macrocyclic amide NH protons were not hydrogen bonded based on the moderate temperature dependence of their chemical shifts ($\Delta\delta/T$ 4.5−7.3 ppb/K).

Solution Structure of Tris-macrocycle 8. Distinguishing features in the ^{1}H NMR spectra of **8** were large $^3J_{\alpha H-NH}$ coupling constants for one Asp(Thz) (9.1 Hz) and two Dap(Ox) (8.2 Hz, 8.2 Hz) residues, and large (Asn, $^3J_{\alpha H-NH}$ 8.1 Hz) and small (Ala, $^3J_{\alpha H-NH}$ 3.0 Hz) coupling constants within the loop regions. By careful examination of $^3J_{\alpha H-\beta H}$ coupling constants for the 2 Asp(Thz) AMX spin systems, in conjunction with NOE intensities from NOESY spectra, it was possible to obtain stereospecific β-proton assignments and thus 2 χ^1 restraints (−60° ± 30°) for these two residues (Figure 4). Additionally, after D_2O exchange the Dap(Ox) residues contain AMX spin systems, which provided another 2 χ^1 restraints (+60° ± 30°) for these two residues.

NOESY spectra at 600 MHz yielded a total of 59 NOE distance restraints (3 strong short range, 24 medium, 32 long range), which, together with the 9 dihedral angle restraints derived from the χ^1 restraints and $^3J_{\alpha H-NH}$ coupling constants, were used in an XPLOR-based NMR solution structure determination. The 10 lowest energy structures of **8** (Figure 5) show a moderately convergent (RMSD 0.43 Å) saddle-shaped macrocyclic scaffold (Figure 5, green) supporting two tripeptide loops (red, blue) that project orthogonally from the same face of the scaffold (Figure 5A). There were no constraining NOEs between the loops, which consequently displayed some variability in their positions (Figure 5B). The loops project from the same face of the macrocycle and are in an eclipsed conformation (Figure 5C). The α−β side-chain vectors of the

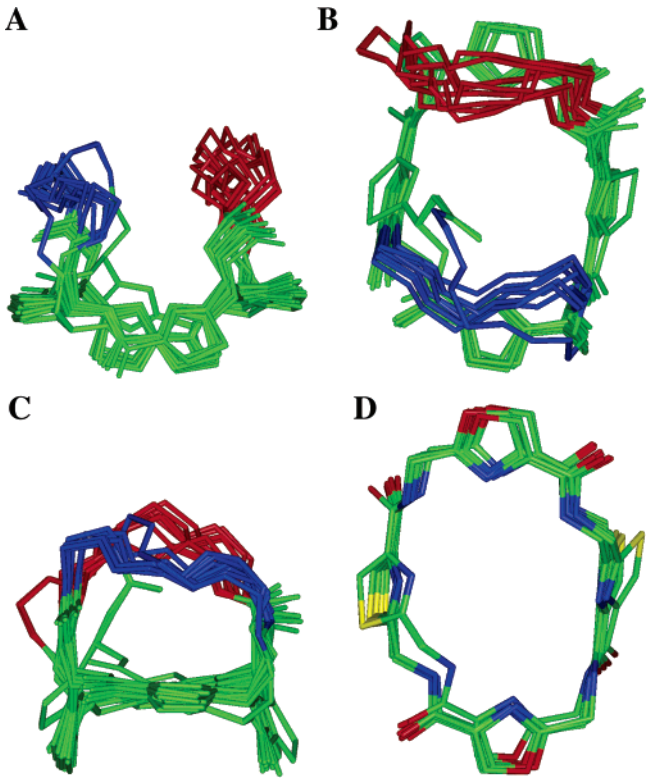

Figure 5. Comparison of 10 lowest energy NMR-derived solution structures superimposed for tricyclic loop assembly **8** in water: (A), end view; (B), top view; (C), side view of backbones (side chains not displayed) showing macrocyclic scaffold including linkers analogous to **6** (green); and Asp−Asn−Ala (blue) and Lys−Gly−Glu (red) loops analogous to cytochrome b_{562}. (D) top view shows the macrocycle with loops omitted.

two Dap-oxazole and two Asp-thiazole units are directed perpendicularly to the macrocycle, which is pseudo-planar (Figure 5C,D). The NMR structure calculation for **8** was highly sensitive to dihedral angle, particularly χ^1 restraints. Additional structure calculations performed without χ^1 restraints (Supporting Information) gave structures with staggered, instead of eclipsed, loop conformations that were of only slightly (2−4 kcal) lower energy.

Comparison between Macrocycles and Cytochrome b_{562}. The macrocycle that is common to **6** and **8** has a slightly different structure in each case. In **6**, it displays a conformationally averaged structure (Figure 3) that is almost planar. In **8**, the loops appear to alter the conformation of the macrocyclic

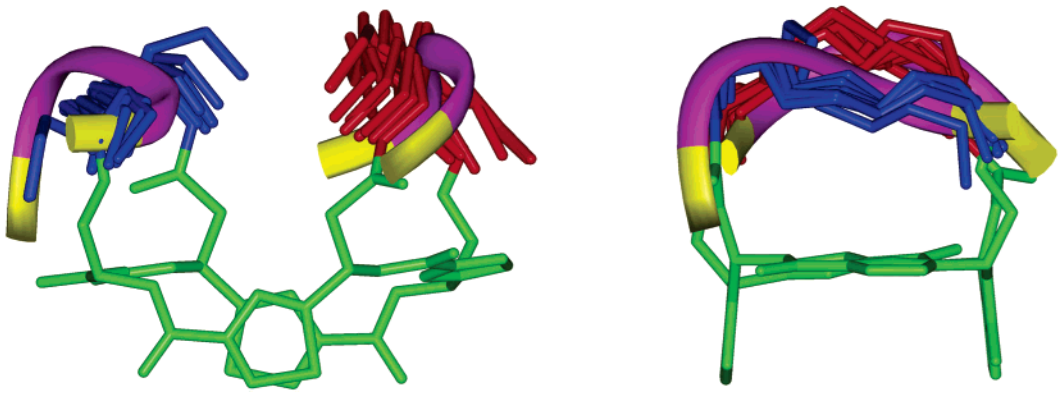

Figure 6. Comparison of loop regions of **8** with those from cytochrome b_{562}. End (left) and side view of an ensemble of 10 NMR solution structures of **8** (only one scaffold (green) shown for clarity) with the backbone loop atoms of Asp21−Asn22−Ala23 (blue) and Glu81−Gly82−Lys83 (red) superimposed onto corresponding loop atoms (purple ribbons) from the crystal structure of cytochrome b_{562}.

scaffold analogous to **6**, making it more saddle shaped (Figure 5). The loops in this solution structure of **8** are not in close contact, as evidenced by the lack of interloop NOEs, and this is similar to the situation observed in the crystal structure of cytochrome b_{562}.[12] In comparison with our reported structure of **7**, involving very short loops[17] that bias the macrocycle toward a rhomboid shape, the larger loops in **8** allow the macrocyclic scaffold to become slightly less rhombohedral and a little squarer. This highlights the fact that the constrained macrocyclic scaffold has some degree of flexibility, despite the presence of four heterocyclic five-membered rings conjugated to four planar amide bonds in the 24-membered cycle, and is susceptible to conformational change induced by the attached loops in **7** and **8**.

InsightII was used to compare the NMR solution structure of **8** with the cytochrome b_{562} crystal structure by superimposing the two tripeptide loop regions. The superimpose function performs a best fit alignment of two structures, calculating the root mean square deviation (RMSD) between corresponding pairs of atoms of a source and target structure. Therefore, the backbone heavy atoms of the tripeptide loops of **8** (source) were superimposed on to the corresponding atoms of cytochrome b_{562} (target). Figure 6 shows a superimposition of all 18 heavy atoms (backbone tripeptide loop atoms, N, Cα, C) from 10 low energy solution structures of **8** onto the corresponding interhelical tripeptide loops from the crystal structure of cytochrome b_{562}. Individually, each loop (9 backbone atoms) of **8** superimposed quite well onto the respective loop atoms in the cytochrome crystal structure (Asp21−Asn22−Ala23 (blue), mean RMSD 0.5 Å; Glu81−Gly82−Lys83 (red), mean RMSD 0.7 Å). In the static crystal structure of the native cytochrome protein, the loop regions are somewhat rigid, being highly constrained by being joined directly to the ends of α-helices, the distance between them varying according to the dynamics of the α-helical bundle. In the case of **8**, the flexible aliphatic components of Dap and Asp linkers provided more mobility to the loops. The combined mean RMSD for both loops of **8** on the cytochrome loops was 2.4 Å.

It is clear that this template approach has successfully anchored the loops of **8** within comparable three-dimensional space to that occupied by the interhelical loops of cytochrome b_{562}. This is consistent with our previous assertion for scaffolds supporting 4-helix bundles,[22] that the geometric requirements of a scaffold do not need very high precision, so long as the scaffold plus linkers permit the peptide surfaces access to the desired three-dimensional space. Although it remains to be determined for specific examples of protein surface mimicry just how much flexibility should be introduced into the scaffold or linkers, we think that some degree of flexibility will generally be necessary to accommodate the induced fit needed for cooperative interactions with proteins that mediate function.

Conclusions

Using dipeptide surrogates H-Dap(Ox)-OH and H-Asp(Thz)-OH and multiple differential protection strategies, we successfully constructed a densely functionalized macrocyclic octapeptide analogue that has proven to be a useful scaffold for creating a protein surface mimetic. Two tripeptide sequences, corresponding to the α1-α2 (Lys21−Gly22−Glu23) and α3-α4 (Asp81−Asn82−Ala83) interhelical loops of cytochrome b_{562}, were sequentially grafted and cyclized onto the differentially protected scaffold by condensation with its Dap and Asp side chains, producing a tris-macrocyclic compound **8**. An NMR-based structure determination revealed that the tris-macrocycle structure in water featured two loops projecting orthogonally from the same face of a saddle-shaped macrocyclic scaffold. Comparison with the crystal structure of cytochrome b_{562} indicated a very good match between the location of each tripeptide loop of **8** and the positions of the corresponding interhelical tripeptide loops defined in the solid-state structure of the cytochrome. The ensemble of solution structures for **8** also indicated some loop flexibility, which may be very important to accommodate the induced fit in protein−protein interactions. However, just how much flexibility and how long the linkers between scaffold and loops need to be in specific protein surface mimetics, to impart optimal interactions with macromolecular receptors, remains to be determined through comparative studies on other protein surface mimics. We conclude that this approach, and even this type of scaffold, appears to be very promising for the structural mimicry of discontinuous loop surfaces of proteins.

Experimental Section

Materials and Methods. Materials obtained commercially were reagent grade unless otherwise stated. Preparative scale reverse phase

(22) Wong, A.; Jacobsen, M. P.; Winzor, D. J.; Fairlie, D. P. *J. Am. Chem. Soc.* **1998**, *120*, 3836−3841.

HPLC separations were performed on a Vydac 218TP101550 C18 column; analytical reverse phase HPLC was performed on a Vydac 218TP54 C18 column [Rt(1)] and Phenomenex Luna 5μ C18 column [Rt(2)], using gradient mixtures of water/0.1%TFA (solvent system A) and water 10%/acetonitrile 90% /TFA 0.1% (solvent system B). Mass spectra were obtained on a hybrid quadrupole TOF mass spectrometer (PE SCIEX API QSTAR Pulsar) equipped with an Ionspray (pneumatically assisted electrospray) operating at ambient temperature (ISMS).

Molecular Modeling. Simulations were performed with InsightII software[23] running on Silicon Graphics R10000 Octane workstations. InsightII modules used were Builder, Search and Compare, Discover and Discover 3. Scaffold **6** was truncated to convert the Lys and Glu side chains into Dap and Asp, and the tripeptide interhelical loops were grafted onto the scaffold using the Builder module. The N-terminus of tripeptide Asp−Asn−Ala was connected to an aspartic acid side chain of modified **6** forming an amide bond, and the C-terminus of the tripeptide connected to the Dap amine side chain of **6** forming a loop that included oxazole. The N-terminus of Glu−Gly−Lys was connected to the other aspartic acid side chain of **6** to form an amide bond, and the C-terminus of this tripeptide was connected to the other Dap amine side chain of **6** to form a second loop that also included oxazole. The resulting structure **8** was then optimized within Builder using default parameters. Force field CFF91 was then selected, and the potentials, partial charges, and formal charges of the **8** were fixed. Discover 3 was then used to perform energy minimization using default parameters and gradient methods. Energy minimization was stopped once the final convergence value reached 0.001. Compound **8** was then subjected to minimization with template forcing constraints (template forcing). Backbone atoms of the flexible tripeptide loop regions of **8** were minimized with template forcing to constrain atoms to the same positions as corresponding backbone atoms of the tripeptide interhelical loops of cytochrome b_{562}. This was performed as described in the InsightII module using a series of decreasing force constraints over the loop tripeptide backbone atoms, repeated until **8** could be minimized without template forcing, to produce a structure with an RMSD of 1.21 Å over the 24 backbone (CO, Cα, N) atoms of **8** and cytochrome b_{562}.

NMR Spectroscopy. ^{1}H, NMR spectra were recorded on a Bruker Avance 600 spectrometer on samples containing 1−4 mM peptide in water at pH 4.0. Proton and carbon assignments were made using TOCSY (80 ms mixing time), DQF-COSY, NOESY (40, 100, 350 ms mixing time), HSQC and HMBC spectra according to the sequential assignment method.[24] Water suppression in 2D experiments was performed using a 3-9-19 Watergate pulse sequence. Variable-temperature 1D ^{1}H and TOCSY spectra were typically collected at 5 K increments from 278 to 313 K. For identification of slowly exchanging amides, a series of 1D ^{1}H and TOCSY spectra were run immediately after dissolving the peptide (3 mg) in D_2O (600 μL). All spectra were analyzed in Xwinnmr.[25]

Structure Calculations. Backbone dihedral angle restraints were derived from $^3J_{\alpha H-NH}$ coupling constants measured from high-resolution 1D ^{1}H NMR spectra. ϕ angles were restrained to $-120° \pm 20°$ for $^3J_{\alpha H-NH} > 8.0$ Hz and to $-60° \pm 20°$ for $^3J_{\alpha H-NH} < 6$ Hz. No explicit hydrogen bonds were used as distance restraints in structure calculations. NOE distance restraints were derived from spectra at 300 K (compound **6**) and 303 K (compound **8**), but lower or higher temperature NOESY spectra were also used to resolve ambiguities arising from NH overlap. Upper distance restraints of 2.7, 3.5, 5.0, and 6.0 Å were used for strong, medium, weak, and very weak nOe's respectively. Stereospecific assignments of β-methylene protons and χ-1 dihedral angles for AMX spin systems (DTZ) were determined by examining $^3J_{H\alpha,H\beta}$ coupling constants in high-resolution 1D ^{1}H NMR before and after D_2O exchange in combination with NOE peak intensities at short mixing times (40, 100, 120 ms). Other diastereotopic protons were not stereospecifically assigned, and corresponding distance restraints were adjusted with standard pseudo-atom corrections.[26] Solution structures were calculated using simulated annealing and energy minimization protocols within XPLOR 3.851.[27] Initial structures were generated using random ϕ,ψ dihedral angles and energy-minimized. Preliminary structures were generated by torsion angle simulated annealing involving a high-temperature (50 000 K) phase comprising 1000 steps of 0.015 ps of torsion angle dynamics, a cooling phase with 1000 steps of 0.015 ps of torsion angle dynamics during which the temperature was lowered to 0 K, and an energy minimization phase comprising 2000 steps of Powell minimization. Typically, 50 structures were calculated, and the 20 structures of lowest energy were superimposed and compared using Insight II.[23]

Structural Superimpositions. InsightII superimposition calculates the root mean square deviation (RMSD) between corresponding pairs of atoms of a source and target structure. For each individual NMR structure of **8**, the tripeptide backbone (N, Cα, CO) atoms of the two loops (24 source atoms) were superimposed on to the corresponding backbone atoms (24 target atoms) of the cytochrome b_{562} crystal structure. The average superimposition RMSD of 10 structures when compared to the crystal structure was 2.4 Å over the 24 backbone atoms of both loops. However, superimposition of the 12 backbone atoms of each loop gave lower average RMSD values of 0.5 Å (Asp−Asn−Ala, α1-α2) and 0.7 Å (Glu−Gly−Lys, α3-α4).

Chemical Synthesis. Cyclo[−Dap(Alloc)(Ox)Asp(OAllyl)(Thz)-Dap(H)(Ox)Asp(O*t*Bu)(Thz)−] (13). Boc-Dap(Fmoc)(Ox)Asp(O*t*Bu)-(Thz)Dap(Alloc)(Ox)Asp(OAllyl)(Thz)-OH (**12a**, 245 g, 0.20 mmol) was stirred with HCO_2H (15 mL) at room temperature for 15 min. The reaction mixture was concentrated under vacuum at ambient temperature, and the residue was purified by rp-HPLC to give TFA·H-Dap-(Fmoc)(Ox)Asp(O*t*Bu)(Thz)Dap(Alloc)(Ox)Asp(OAllyl)(Thz)-OH (**12b**) as a white solid (202 mg, 82%). ISMS: M + H = 1123.3. HRMS: M + H = experimental 1123.3264, calculated 1123.3284. HPLC: Rt(1) = 24.7 min and Rt(2) = 25.9 min, 3.33%/min linear gradient starting from 0% B. TFA·H-Dap(Fmoc)(Ox)Asp(O*t*Bu)(Thz)Dap(Alloc)Asp-(OAllyl)(Thz)-OH (**12b**, 200 mg, 0.16 mmol) and BOP (110 mg, 0.25 mmol) were dissolved in DMF (125 mL) and stirred with DIPEA (0.1 mL, 0.57 mmol) at room temperature for 48 h. The solvent was evaporated in vacuo. The residue was stirred with 30% piperidine/DCM (25 mL) at room temperature for 1 h and purified by rpHPLC to yield cyclo[−Dap(Alloc)(Ox)Asp(OAllyl)(Thz)Dap(H)(Ox)Asp(O*t*Bu)(Thz)−] (**13**) as a white solid (130 mg, 81%). ISMS: M + H = 883.2. HRMS: M + H = experimental 883.2476, calculated 883.2498. HPLC: Rt(1) = 21.1 min and Rt(2) = 22.5 min, 3.33%/min linear gradient starting from 0% B. ^{1}H NMR (DMSO-d_6): δ 8.97, m, 2H, Asp-αNH & Dap-αNH; 8.76, s, 1H, Ox-H; 8.70, d, 1H, $^3J_{AspαNH-AspαH}$ = 8.4 Hz, Asp-αNH; 8.63, s, 1H, Ox-H; 8.53, d, 1H, $^3J_{DapαNH-DapαH}$ = 6.7 Hz, Dap-αNH; 8.27, s, 1H, Thz-H; 8.26, s, 1H, Thz-H; 8.13, br s, 3H, Dap-γNH_3^+; 7.57, t, 1H, $^3J_{Dap\gamma NH-Dap\gamma H}$ = 6.0 Hz, Dap-γNH; 5.85, m, 2H, 2 × H_2C═C**H**−CH_2−O; 5.76, m, 2H, 2 × Asp-αH; 5.70, m, 1H, Dap-αH; 5.26, d, 1H, J = 17.3 Hz, **H**$_2$C═CH−CH_2−O; 5.23, d, 1H, J = 17.4 Hz, **H**$_2$C═CH−CH_2−O; 5.17, d, 1H, J = 10.5 Hz, **H**$_2$C═CH−CH_2−O; 5.15, d, 1H, J = 10.5 Hz, **H**$_2$C═CH−CH_2−O; 5.11, m, 1H, Dap-αH; 4.51, d, 2H, J = 5.0 Hz, ester H_2C═CH−C**H**$_2$−O; 4.44, br s, 2H, Alloc H_2C═CH−C**H**$_2$−O; 3.40−3.62, m, 4H, Dap-βH; 3.34, dd, 2H, J = 12.0, 7.3 Hz, Asp-βH; 3.08, dd, 1H, J = 16.4, 8.6 Hz, Asp-βH; 2.97, dd, 1H, J = 16.4, 6.3 Hz, Asp-βH; 1.30, s, 9H, *t*-Bu. ^{13}C NMR (DMSO-d_6): δ 169.72 (Asp γ-**C**O_2Allyl); 169.68 (Asp γ-**C**O_2*t*Bu); 168.80 (Thz C-2); 168.45 (Thz C-2); 163.22 (Ox C-2); 160.67 (Ox C-2); 160.55 (Thz 4-**C**ONH); 160.36 (Thz 4-**C**ONH); 159.12 (Ox 4-**C**ONH); 159.03 (Ox 4-**C**ONH); 156.24 (Alloc-**C**O);

(23) *InsightII Modeling Environment, Release 2000*; Accelrys Inc., San Diego, CA, 2001.
(24) Wuthrich, K. *NMR of Proteins and Nucleic Acids*; Wiley−Interscience: New York, 1986.
(25) Xwinnmr v2.6 and 3.5, Copyright 2004; Bruker BioSpin GmbH, Rheinstetten, Federal Republic of Germany.
(26) Wuthrich, K.; Billeter, M.; Braun, W. J. *J. Mol. Biol.* **1983**, *169*, 949−961
(27) Brünger, A. T. *X-PLOR Manual Version 3.1*; Yale University, New Haven, CT, 1992.

148.47 (Thz C-4); 148.25 (Thz C-4); 142.66 (Ox C-5); 142.61 (Ox C-5); 136.20 (Ox C-4); 135.60 (Ox C-4); 133.43 (Alloc H_2C═**C**H−CH_2−O); 132.34 (ester H_2C═**C**H−CH_2−O); 126.00 (Thz C-5); 125.01 (Thz C-5); 117.79 (ester H_2**C**═CH−CH_2−O); 117.05 (Alloc H_2**C**═CH−CH_2−O); 80.63 (−CO_2**C**$(CH_3)_3$); 64.63 (H_2C═CH−**C**H_2−O); 64.60 (H_2C═CH−**C**H_2−O); 48.32 (Dap-αCH); 46.40 (Asp-αCH); 45.14 (Asp-αCH); 44.57 (Dap-αCH); 42.28 (Dap-β**C**H_2); 39.50 (Dap-β**C**H_2); 39.08 (Asp-β**C**H_2); 36.63 (Asp-β**C**H_2); 27.53 (−CO_2C(**C**$H_3)_3$.

Compound 14. A solution of cyclo[−Dap(Alloc)(Ox)Asp(OAllyl)-(Thz)-Dap(H)(Ox)Asp(O*t*Bu)(Thz)−] (**13**, 125 mg, 0.13 mmol) and Boc-Glu(OcHx)GlyLys(Z)-OH (136 mg, 0.21 mmol) in DMF (25 mL) was cooled to ∼5 °C under an atmosphere of nitrogen and stirred with a mixture of DPPA (70 μL, 0.33 mmol) and DIPEA (70 μL, 0.4 mmol) for 12 h at the above temperature. The reaction mixture was then warmed to 20 °C and stirred for further 36 h. The solvent was evaporated in vacuo, and the residue was dissolved in water/acetonitrile (1:1, 50 mL), and freeze-dried. ISMS: M + H = 1513.6. The freeze-dried material was stirred with 75% TFA/DCM (20 mL) for 2 h at room temperature. The reaction mixture was concentrated under reduced pressure, and the residue was purified by rpHPLC to give **14** as a white solid (155 mg, 84%). ISMS: M + H = 1357.5. HRMS: M + H = experimental 1357.4621, calculated 1357.4612. HPLC: Rt(1) = 23.6 min and Rt(2) = 24.8 min, 3.33%/min linear gradient starting from 0% B. ^{1}H NMR (DMSO-d_6): δ 8.84, d, 1H, $^3J_{\mathrm{Asp\alpha NH-Asp\alpha H}}$ = 8.7 Hz, Asp-αNH; 8.79, d, 2H, $^3J_{\mathrm{\alpha NH-\alpha H}}$ = 8.6 Hz, Asp-αNH & Dap-αNH; 8.76, d, 1H, $^3J_{\mathrm{Dap\alpha NH-Dap\alpha H}}$ = 8.6 Hz, Dap-αNH; 8.61−8.63, m, 3H, 2 × Ox-H & Gly-αNH; 8.34, m, 1H, Dap-γNH; 8.25, s, 2H, 2 × Thz-H; 8.13, br s, 3H, Glu-αNH_3^+; 8.07, d, 1H, $^3J_{\mathrm{LysNH-Ly s\alpha H}}$ = 8.2 Hz, Lys-αNH; 7.56, t, 1H, $^3J_{\mathrm{Dap\gamma NH-Dap\gamma H}}$ = 5.6 Hz, Dap-γNH; 7.29−7.38, m, 5H, Ar−H; 7.17, t, 1H, $^3J_{\mathrm{Lys\epsilon NH-Lys\epsilon H}}$ = 5.7 Hz, Lys-ϵNH; 5.82, m, 2H, H_2C═C**H**−CH_2−O; 5.77, m, 1H, Asp-αH; 5.71, m, 1H, Asp-αH; 5.40, m, 1H, Dap-αH; 5.37, m, 1H, Dap-αH; 5.24, dd, 1H, J = 15.6, 1.7 Hz, **H**$_2$C═CH−CH_2−O; 5.21, dd, 1H, J = 12.1, 1.6 Hz, **H**$_2$C═CH−CH_2−O; 5.15, dd, 1H, J = 10.5, 1.4 Hz, **H**$_2$C═CH−CH_2−O; 5.11, dd, 1H, J = 10.5, 1.4 Hz, **H**$_2$C═CH−CH_2−O; 5.00, s, 2H, PhC**H**$_2$; 4.67, m, 1H, cyclohexyl C**H**−O; 4.52, d, 2H, J = 4.6 Hz, ester H_2C═CH−C**H**$_2$−O; 4.44, br s, 2H, Alloc H_2C═CH−C**H**$_2$−O; 4.16, m, 1H, Lys-αH; 3.91, m, 1H, Dap-βH; 3.84−3.89, m, 2H, Gly-αH & Glu-αH; 3.75−3.80, m, 2H, Gly-αH & Dap-βH; 3.53, m, 1H, Dap-βH; 3.45, m, 1H, Dap-βH; 3.00−3.26, m, 4H, Asp-βH; 2.89, m, 2H, Lys-ϵH; 2.43, m, 2H, Glu-γH; 1.97, m, 2H, Glu-βH; 1.75, m, 2H, cyclohexyl-H; 1.64, m, 2H, cyclohexyl-H; 1.45−1.52, m, 3H, Lys-βH & 2 × cyclohexyl-H; 1.27−1.41, m, 5H, Lys-βH, 2 × cyclohexyl-H & 2 × Lys-δH; 1.10−1.24, m, 4H, 2 × Lys-γH & 2 × cyclohexyl-H.

Compound 15. A solution of **14** (150 mg, 0.10 mmol) in DMF (110 mL) was cooled to ∼5 °C under an atmosphere of nitrogen and stirred with a mixture of DPPA (70 μL, 0.33 mmol) and DIPEA (62 μL, 0.36 mmol) for 42 h. The solvent was evaporated under vacuum, and the residue was freeze-dried. ISMS: M + H = 1339.5. The freeze-dried material was dissolved in dichloromethane (20 mL) and stirred with a mixture of $Pd(PPh_3)_4$ (cat.), 1,3-dimethylbarbituric acid (88 mg, 0.55 mmol, 98%), and acetic acid (8 μL, 0.14 mmol) under an atmosphere of nitrogen and in the absence of light for 2 h. The solvent was removed under reduced pressure, and the residue was purified by rp-HPLC to give **15** as a white solid (116 mg, 86%). ISMS: M + H = 1215.4. HRMS: M + H = experimental 1215.3962, calculated 1215.3982. HPLC: Rt(1) = 21.4 min and Rt(2) = 22.6 min, 3.33%/min linear gradient starting from 0% B. ^{1}H NMR (DMSO-d_6): δ 8.94, d, 1H, $^3J_{\mathrm{Dap\alpha NH-Dap\alpha H}}$ = 8.6 Hz, Dap-αNH; 8.88, d, 1H, $^3J_{\mathrm{Asp\alpha NH-Asp\alpha H}}$ = 8.2 Hz, Asp-αNH; 8.82, d, 1H, $^3J_{\mathrm{Dap\alpha NH-Dap\alpha H}}$ = 9.0 Hz, Dap-αNH; 8.66, s, 1H, Ox-H; 8.44, d, 1H, $^3J_{\mathrm{Asp\alpha NH-Asp\alpha H}}$ = 8.9 Hz, Asp-αNH; 8.37, s, 1H, Ox-H; 8.29, s, 1H, Thz-H; 8.20, s, 1H, Thz-H; 8.11, m, 2H, Glu-αNH & Dap-γNH; 8.03, m, 4H, Lys-αNH & Dap-$\gamma$$NH_3^+$; 7.80, m, 1H, Gly-αNH; 7.25−7.40, m, 5H, Ar−H; 7.22, t, 1H, $^3J_{\mathrm{Lys\epsilon NH-Lys\epsilon H}}$ = 5.8 Hz, Lys-ϵNH; 5.71, m, 1H, Asp-αH; 5.65, m, 2H, Asp-αH & Dap-αH; 5.59, m, 1H, Dap-αH; 5.00, s, 2H, PhC**H**$_2$; 4.64, m, 1H, cyclohexyl C**H**−O; 4.42, m, 1H, Glu-αH; 3.90−3.97, m, 2H, Gly-αH & Lys-αH; 3.74, m, 1H, Dap-βH; 3.41−3.55, m, 4H, 3 × Dap-βH & Gly-αH; 3.00−3.17, m, 4H, Asp-βH; 2.95, m, 2H, Lys-ϵH; 2.25, m, 2H, Glu-γH; 1.92, m, 1H, Glu-βH; 1.73, m, 3H, Glu-βH & 2 × cyclohexyl-H; 1.65, m, 2H, cyclohexyl-H; 1.57, m, 1H, Lys-βH; 1.47, m, 2H, Lys-βH & Lys-δH; 1.28−1.38, m, 7H, Lys-δH & 6 × cyclohexyl-H; 1.14−1.24, m, 2H, Lys-γH.

Compound 16. A mixture of Boc-Asp(OcHx)Asn(NHTrt)Ala-OH (86 mg, 0.12 mmol), DPPA (25 μL, 0.12 mmol), and DIPEA (21 μL, 0.12 mmol) in DMF (5 mL) was stirred at ∼5 °C for 15 min and then added to a solution of **15** (60 mg, 0.045 mmol) and DIPEA (15.8 μL, 0.091 mmol) in DMF (10 mL) at ∼5 °C under an atmosphere of nitrogen. The stirring was continued at this temperature for 4 days. The reaction mixture was concentrated, and the residue was freeze-dried. ISMS: M + H = 1939.7. The freeze-dried material was stirred with 75% TFA/DCM (20 mL) for 2 h at room temperature. The reaction mixture was concentrated under reduced pressure, and the residue was purified by rpHPLC to give **16** as a white solid (50.2 mg, 65%). ISMS: M + H = 1597.6. HRMS: M + H = experimental 1597.5821, calculated 1597.5835. HPLC: Rt(1) = 22.8 min and Rt(2) = 23.7 min, 3.33%/min linear gradient starting from 0% B. ^{1}H NMR (DMSO-d_6): δ 8.93, d, 1H, $^3J_{\mathrm{Dap\alpha NH-Dap\alpha H}}$ = 7.6 Hz, Dap-αNH; 8.80, d, 1H, $^3J_{\mathrm{Dap\alpha NH-Dap\alpha H}}$ = 8.5 Hz, Dap-αNH; 8.63, s, 1H, Ox-H; 8.60, m, 2H, Ox-H & Glu-αNH; 8.56, d, 1H, $^3J_{\mathrm{Asp\alpha NH-Asp\alpha H}}$ = 7.6 Hz, Asp-αNH; 8.48, d, 1H, $^3J_{\mathrm{Asp\alpha NH-Asp\alpha H}}$ = 7.5 Hz, Asp-αNH; 8.29, s, 1H, Thz-H; 8.25, s, 1H, Thz-H; 8.11, m, 2H, Dap-γNH & Asn-αNH; 8.02, m, 1H, Gly-αNH; 7.95, m, 4H, Ala-αNH & Asp-NH_3^+; 7.90, d, 1H, $^3J_{\mathrm{Lys\alpha NH-Lys\alpha H}}$ = 7.6 Hz, Lys-αNH; 7.81, t, 1H, $^3J_{\mathrm{Dap\gamma NH-Dap\gamma H}}$ = 5.6 Hz, Dap-γNH; 7.51, br s, 1H, Asn-CONH; 7.25−7.37, m, 5H, Ar−H; 7.19, t, 1H, $^3J_{\mathrm{Lys\epsilon NH-Lys\epsilon H}}$ = 5.7 Hz, Lys-ϵNH; 6.97, br s, 1H, Asn-CONH; 5.90, m, 1H, Asp-αH; 5.48−5.54, m, 3H, 2 × Dap-αH & Asp-αH; 5.00, s, 2H, $PhCH_2$; 4.63, m, 2H, cyclohexyl CH−O; 4.32, m, 1H, Asn-αH; 3.88−4.15, m, 6H, Glu-αH, 2 × Asp-βH, Ala-αH, Dap-βH & Lys-αH; 3.69, m, 2H, Gly-αH & Dap-βH; 3.56, m, 2H, Gly-αH & Dap-βH; 3.34−3.48, m, 4H, 2 × Dap-βH & 2 × Asp-βH; 3.10−3.27, m, 2H, Asp-βH; 2.96, m, 2H, Lys-ϵH; 2.79−2.90, m, 2H, Asp-βH; 2.55−2.67, m, 2H, Asn-βH; 2.38, m, 1H, Glu-γH; 2.27, m, 1H, Glu-γH; 1.98, m, 1H, Glu-βH; 1.87, m, 1H, Glu-βH; 1.74, m, 2H, cyclohexyl-H; 1.64, m, 2H, cyclohexyl-H; 1.55, m, 1H, Lys-βH; 1.47, m, 2H, Lys-βH & cyclohexyl-H; 1.16−1.40, m, 9H, 2 × Lys-δH, 5 × Cyclohexyl-H & 2 × Lys-γH; 1.08, d, 3H, J = 7.2 Hz, Ala-βH.

Compound 8. A solution of **16** (42 mg, 0.025 mmol) in DMF (40 mL) was cooled to ∼5 °C and stirred with a mixture of DPPA (15 μL, 0.07 mmol) and DIPEA (15 μL, 0.086 mmol) under an atmosphere of nitrogen for 48 h. The reaction mixture was then allowed to warm to ∼25 °C and stirred for further 8 days. The solvent was evaporated under reduced pressure at ambient temperature, and the residue was purified by rp-HPLC to give the protected tris-macrocycle as a white solid in quantitative yield. ISMS: M + H = 1579.6. HRMS: M + H = experimental 1579.5746, calculated 1579.5729. HPLC: Rt(1) = 24.5 min and Rt(2) = 26.4 min, 3.33%/min linear gradient starting from 0% B. The protected tris-macrocycle (12 mg, 8.2 × 10^{-6} mol) was treated with HF in the presence of *p*-cresol and purified by rp-HPLC to give **8** as a white solid (4 mg, 35%). ISMS: M + H = 1281.4. HRMS: M + H = experimental 1282.3776, calculated 1281.3796. HPLC: Rt(1) = 14.8 min and Rt(2) = 15.9 min, 3.33%/min linear gradient starting from 0% B. ^{1}H NMR (H_2O/D_2O, 303 K): δ 9.37, d, 1H, $^3J_{\mathrm{Asp(Thz)NH-Asp(Thz)\alpha H}}$ = 9.1 Hz, Asp(Thz)3-αNH; 8.92, d, 1H, $^3J_{\mathrm{Asp(Thz)NH-Asp(Thz)\alpha H}}$ = 8.1 Hz, Asp(Thz)1-α NH; 8.91, d, 1H, $^3J_{\mathrm{AspNH-Asp\alpha H}}$ = 6.9 Hz, Asp-αNH; 8.90, d, 1H, $^3J_{\mathrm{Dap(Ox)NH-Dap(Ox)\alpha H}}$ = 8.2 Hz, Dap-(Ox)4-αNH; 8.70, d, 1H, $^3J_{\mathrm{Dap(Ox)NH-Dap(Ox)\alpha H}}$ = 8.2 Hz, Dap(Ox)2-α NH; 8.58, d, 1H, $^3J_{\mathrm{GluNH-Glu\alpha H}}$ = 7.4 Hz, Glu-αNH; 8.389, s, 1H, Ox-H; 8.387, s, 1H, Ox-H; 8.35, d, 1H, $^3J_{\mathrm{AlaNH-Ala\alpha H}}$ = 4.8 Hz, AlaNH; 8.33, m, 1H, Dap(Ox)4-γNH; 8.31, m, 1H, Dap(Ox)2-γNH; 8.24, t, 1H, $^3J_{\mathrm{GlyNH-Gly\alpha H}}$ = 6.3 Hz, Gly-αNH; 8.21, s, 1H, Thz-H; 8.207, s, 1H, Thz-H; 8.11, d, 1H, $^3J_{\mathrm{DapNH-Dap\alpha H}}$ = 7.1 Hz, LysαNH; 7.81, d,

1H, $^3J_{\mathrm{AsnNH-Asn\alpha H}}$ = 8.1 Hz, Asn-αNH; 7.69, s, 1H, Asnδ NH; 7.51, br s, 3H, Lys-zNH_3; 6.91, s, 1H, Asnδ NH; 6.06, m, 1H, Asp(Thz)3-αH;, 5.69, m, 1H, Asp(Thz)1-αH; 5.46, m, 1H, Dap(Ox)4-αH; 5.39, m, 1H, Dap(Ox)2-αH; 4.65, m, 1H, Asn-αH; 4.50, m, 1H, Glu-αH; 4.49, m, 1H, Asp-αH; 4.18, m, 1H, Lys-αH; 4.16, m, 1H, Dap(Ox)2-β H; 4.03, m, 1H, Ala-αH; 3.98, m, 1H, Asp(Thz)1-β H; 3.97, m, 1H, Dap(Ox)4-β H; 3.96, m, 1H, Gly-αH; 3.88, m, 1H, Gly-αH; 3.85, m, 1H, Dap-(Ox)4-β H; 3.71, dd, 1H, $^2J_{\mathrm{Dap\beta H-Dap\beta H}}$ 16.4 Hz, $^3J_{\mathrm{Dap\beta H-Dap\alpha H}}$ = 11.5 Hz, Asp(Thz)3-β H; 3.64, m, 1H, Dap(Ox)2-β H; 3.18, dd, 1H, $^2J_{\mathrm{Dap\beta H-Dap\beta H}}$ 14.7 Hz, $^3J_{\mathrm{Dap\beta H-Dap\alpha H}}$ 3.6 Hz, Asp(Thz)1-β H; 3.11, dd, 1H, $^2J_{\mathrm{Dap\beta H-Dap\beta H}}$ 16.4 Hz, $^3J_{\mathrm{Dap\beta H-Dap\alpha H}}$ 3.0 Hz, Asp(Thz)3-β H; 3.05, m, 1H, Asp-β H; 3.00, m, 2H, Lys-ϵH; 2.81, m, 1H, Asp-β H; 2.51, m, 1H, Asn-β H; 2.50, m, 2H, Glu-γH; 2.14, m, 1H, Glu-β H; 2.10, m, 1H, Asn-β H; 2.02, m, 1H, Glu-β H; 1.80, m, 1H, Lys-β H; 1.66, m, 2H, Lys-δH; 1.66, m, 1H, Lys-β H; 1.44, m, 1H, Lys-γH; 1.37, m, 1H, Lys-γH; 1.27, d, 7.4 Hz, Ala-β H.

Acknowledgment. We thank the ARC and NHMRC for financial support and the ARC Special Research Centre for Functional and Applied Genomics for technical advice.

Supporting Information Available: Further details of chemical synthesis and compound characterization; 1D and 2D NMR spectra for **6**, **8**, **13**, and **14**; structure calculations, variable-temperature NMR data, D_2O exchange data for **6** and **8** (Figures S1−S14); tables of NOE distance and dihedral angle restraints for **6** and **8**, RMSD comparisons of structures for **8** with cytochrome b_{562} (Tables S1−S3). This material is available free of charge via the Internet at http://pubs.acs.org.

JA0455300